Synthesis, Structures, and Thermal Expansion of the La$_2$W$_{2-x}$Mo$_x$O$_9$ Series

J. A. Collado, M. A. G. Aranda, A. Cabeza, P. Olivera-Pastor, and S. Bruque[1]

Departamento de Química Inorgánica, Universidad de Málaga, 29071-Málaga, Spain

The La$_2$W$_{2-x}$Mo$_x$O$_9$ series has been synthesized by the ceramic method. An alternative synthesis using microwave radiation is also reported. La$_2$W$_2$O$_9$ has two polymorphs and the low-temperature phase (α) transforms to the high-temperature form (β) at 1077°C. The influence of the W/Mo substitution in this phase transition has been investigated by DTA. The β structure for $x \geq 0.7$ compositions can be prepared as single phase at any cooling rate. The β phase for $0.3 \leq x \leq 0.7$ compounds can be prepared as single phase by quenching, whereas a mixture of α and β phases is obtained by slow cooling. The W/Mo ratio in both coexisting phases is different with the β-phase having a higher Mo content. The $x = 0.1$ and 0.2 compounds have been prepared as mixtures of phases. The room temperature structure of β-La$_2$W$_{1.7}$Mo$_{0.3}$O$_9$ has been analyzed by the Rietveld method in $P2_13$ space group. The final R-factors were $R_{WP} = 9.0\%$ and $R_F = 5.6\%$ with a structure similar to that of β-La$_2$Mo$_2$O$_9$. Finally, the thermal expansion of both types of structures has been determined from a thermodiffractometric study. The thermal expansion coefficients were 2.9×10^{-6} and 9.7×10^{-6}°C^{-1} for α-La$_2$W$_2$O$_9$ and β-La$_2$W$_{1.2}$Mo$_{0.8}$O$_9$, respectively. © 2002 Elsevier Science (USA)

Key Words: phase transition; low thermal expansion materials; microwave synthesis.

INTRODUCTION

Lone pair substitution (LPS) concept is a new way to looking for oxide ion conductors (1). It is based on the substitution of an element that contains a lone pair by another without it. This promotes the appearance of free spaces (vacancies) in the structure. Moreover, the aliovalent substitution using elements with higher valences can increase the oxide presence to balance the charges. Rare-earth molybdates form an interesting family of compounds with relevant physical properties (2–9). La$_2$Mo$_2$O$_9$ is being intensively studied (9–12) because it is a fast oxide ion

conductor, which exhibits an ionic conductivity as high as 6×10^{-2} S cm^{-1} at 800°C. This value is similar to those of other electrolytes like doped perovskites (13–15), YSZ (16), pyrochlores (17, 18) or BIMEVOX (19, 20).

The crystal structure of β-La$_2$Mo$_2$O$_9$ is related to that of SnWO$_4$. This oxide could be reformulated as Sn$_2$W$_2$O$_8$L$_2$ where L is the lone pair of Sn^{2+}. In La$_2$Mo$_2$O$_9$, molybdenum replaces tungsten and Sn^{2+} is substituted by La^{3+} (without lone pair). So, the lone pair site remains as a vacancy or can be occupied by oxide anions due to the higher valence of La^{3+}. The structural formula of lanthanum molybdate can be rewritten as La$_2$Mo$_2$O$_{8+1}$□ (where □ is a vacancy). The extra-oxide anions can migrate through the vacancies justifying its high conductivity.

La$_2$Mo$_2$O$_9$ exhibits at least two different structures, although a unique atomic framework. β-La$_2$Mo$_2$O$_9$ is the high-temperature (HT) polymorph which is cubic ($P2_13$ space group). α-La$_2$Mo$_2$O$_9$ is the low-temperature (LT) polymorph which seems to exhibit a $2 \times 3 \times 4$ super-structure of the cubic form and is suspected to be monoclinic due to a slight distortion (12). A reversible α-to-β-phase transition occurs around 580°C (11). Several cations substitutions have been tested in La$_2$Mo$_2$O$_9$ by replacing both La and Mo. Mo^{6+} has been substituted by W^{6+} and this stabilizes the β-structure at room temperature (RT) although a crystal structure refinement was not reported and the solid solution limits were also not studied (11).

The corresponding lanthanum and tungsten mixed oxide, La$_2$W$_2$O$_9$, has also been reported (21–24). La$_2$W$_2$O$_9$ presents two different structures (25). A phase transition was reported close to 1070°C. β-La$_2$W$_2$O$_9$, the HT polymorph, was suspected to be cubic with a crystal structure similar to that of β−La$_2$Mo$_2$O$_9$, although this has not been corroborated by a structural study. The triclinic structure of α-La$_2$W$_2$O$_9$ has been very recently determined *ab initio* from neutron powder diffraction data (26) being completely different from that of α-La$_2$Mo$_2$O$_9$. α-Lanthanum tungstate oxide has isolated [W$_4$O$_{18}$]$^{12-}$ groups

[1] To whom correspondence should be addressed. Fax: +34-952-132000. E-mail: bruque@uma.es.

alternating with [WO$_5$] trigonal bipyramids generating a 3D framework with lanthanum atoms in both 9- and 10-fold oxygen polyhedra (26). The α–β–phase transition for La$_2$Mo$_2$O$_9$ at 580°C is displacive, whereas the α–β transition for La$_2$W$_2$O$_9$ at 1070°C is reconstructive.

On the other hand, some tungsten mixed oxides display very low and even negative thermal expansion coefficients. For instance, ZrW$_2$O$_8$ has a thermal expansion coefficient of -8.7×10^{-6} K^{-1} (27–29). The isomorphous replacement of W by Mo in this material was also reported (30). Other related tungstate and molybdate compounds with very low thermal expansion are the A_2M_3O$_{12}$ oxides (where A is a trivalent cation such as Sc or Al and M is a hexavalent cation such as W or Mo). For instance, Sc$_2M_3$O$_{12}$ (M = Mo, W) have negative thermal expansion coefficients (31).

Finally, in the last years, some inorganic materials have been synthesized using microwave radiation (32–34). This reaction requires much shorter reaction times, is simpler and clean. In this article we report the ceramic synthesis of La$_2$W$_{2-x}$Mo$_x$O$_9$ series together with an alternative way using microwave radiation.

The structural consequences of partial substitution of W^{6+} by Mo^{6+} have been studied including the influence in the phase transition. We also report some low thermal expansion data.

EXPERIMENTAL SECTION

Synthesis

(1) Ceramic. The La$_2$W$_{2-x}$Mo$_x$O$_9$ (x = 0, 0.1, 0.2, 0.3, 0.4, 0.5, 0.6, 0.7, 0.8, 1.0, 1.2, 1.4, 1.6, 1.8, 2.0) series was prepared from the appropriated mixtures of La$_2$O$_3$, MoO$_3$ and WO$_3$. Lanthanum oxide was heated at 1000°C for 2 h prior to use for decarbonation. The oxides were mixed in an agate mortar and pelletized. Firstly, the pellets were heated at 500°C for 6 h, then grounded, pelletized and finally calcined at 1100°C for 6 h. Different thermal cooling rates, such as quenching or slow cooling, were used in order to obtain the low- or high-temperature phases.

(2) By microwave radiation. The same starting oxides were mixed, pelletized and embedded in ultrapure graphitic carbon, with a small particle size, in a silica crucible. Approximately 0.1 g of graphite is used for 1 g of sample. The system was irradiated with microwaves in a domestic microwave oven at 2.45 GHz with a power of 900 W during 5 min. This procedure is based on that described by Rao and Selvan. (36) for obtaining GaAlO$_3$. These materials have not been used for the structural studies.

X-Ray Diffraction

The XRPD patterns were collected on a D5000 diffractometer with ($\theta/2\theta$) Bragg-Brentano geometry using graphite monochromatic Cu$K\alpha_{1,2}$ radiation. The XRD patterns were recorded between 16° and 120° in 0.03° steps counting for 15 s for structural characterization. Shorter counting times (4 s) and 2θ range (16–60°) were used for determining the unit cells. The structural studies were carried out by the Rietveld method (37) using the GSAS package. The thermodiffractometries were recorded in the same D5000 apparatus but in a second goniometer equipped with an HTK 10 heating chamber. The patterns were collected between 25°C and 1000°C in He flow over the 10–35° angular range (2θ), with a step size of 0.04° and counting for 5 s.

Thermal Analysis

Differential Thermal Analysis (DTA) data were recorded on a Setaram Labsys Thermal Analyzer. The temperature was varied from RT up to 1200°C at a heating rate of 10 K min^{-1} with calcined Al$_2$O$_3$ as reference.

RESULTS AND DISCUSSION

Syntheses of α and β Polymorphs

The RT polymorph of La$_2$W$_2$O$_9$ is the α form (triclinic) (26). The α-to-β reconstructive phase transition (triclinic to cubic) for stoichiometric La$_2$W$_2$O$_9$ has been measured at 1077°C by DTA. This is in good agreement with the previous reported values (1067°C (25) and 1075°C (23)). Stoichiometric La$_2$W$_2$O$_9$ is obtained as single phase with α-structure at all tested cooling rates. Several quenching treatments, including cooling from 1400°C to liquid nitrogen, were carried out for x = 0.1, and 0.2 compositions in order to obtain the β form as single phase at RT. All attempts were unsuccessful and a mixture of α and β phases was invariably obtained.

For $x \geq 0.3$, the β structure can be prepared as single phase at RT by fast cooling. It is possible to stabilize the β structure (for x = 0.3, 0.4 and 0.5 compositions) by quenching from 1100°C in liquid nitrogen. The slow cooling for these compositions led to a mixture of α and β phases. For x = 0.6 and 0.7 compositions, the β structure is readily obtained by slow cooling (turning off the furnace) although a small amount of α phase can be obtained. For compositions with $x \geq 0.7$, only the β structure is obtained.

α-La$_2$Mo$_2$O$_9$ has been described as a superstructure of the cubic, simpler and disordered, β structure. For x = 1.6 and 1.8 materials, no superstructure peaks are evident in the RT X-ray diffraction patterns. So, the high-temperature cubic structure is stabilized by partial replacement of Mo by W. Furthermore, the DTA data do not show any endothermic peak ruling out a phase transition.

Microwave Synthesis

Some stoichiometries ($x = 2, 1.5, 1, 0.5$) were obtained by the microwave method. The color of the samples were pale gray. The X-ray powder patterns for these materials are displayed in Fig. 1. The pattern for $x = 0.5$ sample has a slightly more irregular background. This synthetic methodology presents three main advantages: firstly, it is fast (the reaction is completed in 5 min); secondly, it is easy and finally, it is economical. The actual problems are the possible presence of inhomogeneities in the products, due to the graphite, that darkens the samples. The graphite impurities can be removed by heating the samples in air at 1000°C for 1 h. This last heating treatment also improves the crystallinity of the microwave-synthesized samples. No W/Mo reduction by carbon during the synthesis has been observed.

Evolution of Phase Transition Temperature in the Series

The α-to-β-phase transition for samples with α phase (slowly cooled) has been characterized by DTA. Fig. 2 shows the DTA curves for $La_2W_{2-x}Mo_xO_9$ ($x = 0, 0.1, 0.2, 0.3, 0.4, 0.5, 0.6$) series. The transition temperature decreases as the Mo content increases. For higher x values, no peaks were found as the samples already crystallizes in the β phase at RT. The endotherms become broader with the Mo content reflecting the smaller amount of α phase in the mixtures and its possible heterogeneity.

Coexistence of α and β Structures

α and β structures can coexist between 0.1 and 0.7 compositions. In this case, we have investigated the Mo content of the phases as two possibilities can be considered:
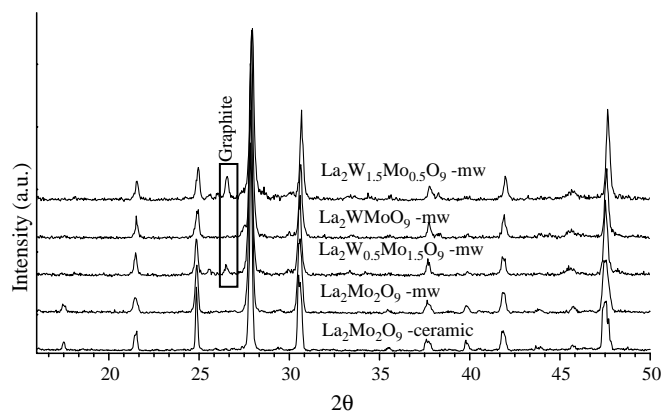
FIG. 2. DTA curves for $La_2W_{2-x}Mo_xO_9$ ($x = 0, 0.1, 0.2, 0.3, 0.4, 0.5, 0.6$) compositions where the α to β-phase transition takes place on heating.

both structures have the same composition or they may have different Mo/W contents.

In order to determine that, we have studied the evolution of the cell parameter, **a**, of the β-phase for single-phase compounds ($x \geq 0.3$ quenched). The evolution along the β-series is well described by a linear fit (Vergard law) in the 0.3–1.0 compositional range (see Fig. 3). For compositions with x larger than 1.0, a change in the linear behavior is observed in agreement with a previous report (11). This linear fit, for x between 0.3 and 1.0, demonstrates that a solid solution is readily obtained for the high-temperature β phase. In this structure, Mo^{6+} behaves with a size slightly larger than W^{6+}. This is not common, but it has been previously reported, for example in $BaXO_4$ ($X = W$ and Mo) (38).

The samples with nominal compositions ($0.3 \leq x \leq 0.7$) and coexistence of α and β phases have also been studied. For these compounds, the diffraction peaks due to the β phase can be extracted and the unit-cell parameter determined. Introducing the a parameter obtained for the nominal x value (x_i) in the linear fit, we can obtain a real x value (x_r) of the β phase. Slowly cooled $La_2W_{1.7}Mo_{0.3}O_9$

FIG. 1. Laboratory X-ray powder diffraction patterns for $La_2W_{2-x}Mo_xO_9$ ($x = 2, 1.5, 1, 0.5$) obtained by the microwave method. The pattern for ceramic ($x = 2$) sample is shown for comparison.
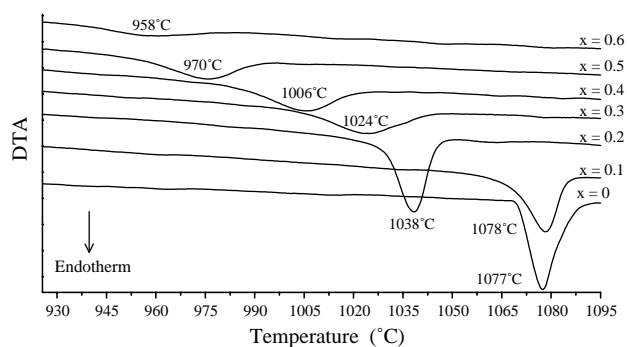
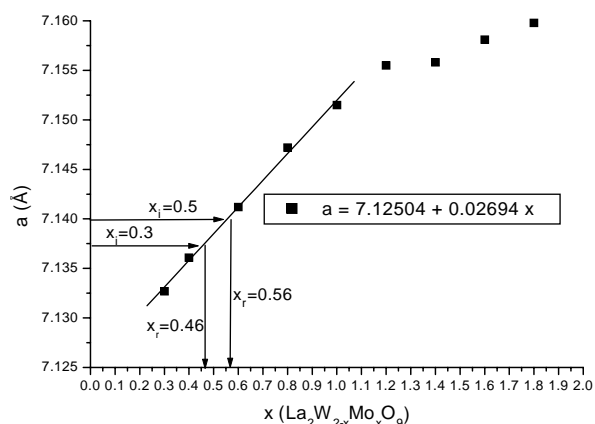**FIG. 3.** Cell parameter variation with x for β-$La_2W_{2-x}Mo_xO_9$ single phases. The interpolation of the cell parameters for β-phases ($x = 0.3$ and 0.5) showing phase coexistence are also shown.

TABLE 1
Crystallographic Parameters for β-La$_2$W$_{1.7}$Mo$_{0.3}$O$_9$ (T = RT, a = 7.13267(5) Å) in Space Group $P2_1$3. Data for β-La$_2$Mo$_2$O$_9$ (T = 617°C, a = 7.2014(5) Å) (Model B) Are Taken from Reference 11 and Showed for Comparison

Atom/position	(Site)	La$_2$W$_{1.7}$Mo$_{0.3}$O$_9$	La$_2$Mo$_2$O$_9$
La (4a)	x	0.8584(2)	0.8509(5)
(xxx)	Occ.	1	1
	U_{iso}/Å^2	0.044(1)	0.062(5)
Mo/W (4a)	x	0.1661(2)	0.166(2)
	Occ.	0.15/0.85	1.00/-
	U_{iso}/Å^2	0.053(1)	0.056(3)
O1 (4a)	x	0.311(1)	0.312(2)
	Occ.	1	1
	U_{iso}/Å^2	0.14(1)	0.099(5)
O2 (12b)	x	0.994(2)	0.987(1)
(xyz)	y	0.184(2)	0.179(3)
	z	0.357(2)	0.332(3)
	Occ.	0.82(1)	0.82(2)
	U_{iso}/Å^2	0.14(1)	0.11(1)
O3 (12b)	x	0.798(1)	0.923(4)
	y	0.610(2)	0.621(6)
	z	0.575(2)	0.558(4)
	Occ.	0.34(2)	0.34(2)
	U_{iso}/Å^2	0.14(1)	0.13(1)

compound (x_i = 0.3) had a β phase with a = 7.137(1) Å that corresponds to x_r = 0.45. So, the β phase is richer in Mo and consequently, the α-phase should be poorer. Similarly, for x_i = 0.5, we obtain x_r = 0.56. These results clearly indicate that the coexisting α and β phases have different W/Mo ratios and that the Mo substitution in α-La$_2$W$_{2-x}$Mo$_x$O$_9$ is rather limited.

Taking together the powder diffraction study and the thermal data, we conclude that Mo is replacing W in the α phase (the transition temperature changes) but this incorporation is smaller than the nominal starting stoichiometry. Probably, a low-temperature 'chimie douce' synthesis is needed in order to obtain a single phase of Mo-substituted α-La$_2$W$_2$O$_9$.

β-Structure

Three stoichiometries [La$_2$W$_{2-x}$Mo$_x$O$_9$ x = 0.3, 0.6 and 0.8] have been structurally characterized. These compounds crystallize in a β structure similar to that of the molybdate end-member. The results were similar, so, we report only the structural details for La$_2$W$_{1.7}$Mo$_{0.3}$O$_9$ which must have a structure quite close to that of β La$_2$W$_2$O$_9$ at RT which is still unknown. We have used the β La$_2$Mo$_2$O$_9$ structure (11, 12) as starting model in the $P2_1$3 space group. The structure of β La$_2$Mo$_2$O$_9$ is disordered and several models for the disorder were tested, including cation deficiencies, (12) because they used neutron powder diffraction data. However, with only laboratory X-ray powder diffraction data we cannot test such models. Hence, we compare the model B of Goutenoire *et al.* for β-La$_2$Mo$_2$O$_9$ (12) with the structure refined by us for La$_2$W$_{1.7}$Mo$_{0.3}$O$_9$ under similar constraints. The final R-factors for β-La$_2$W$_{1.7}$Mo$_{0.3}$O$_9$ were R_{WP} = 9.0%, R_p = 6.7% and R_F = 5.6%. The structural data are given in Table 1 and the Rietveld plot is displayed in Fig. 4.

From the data reported in Table 1, we conclude that the structure of β-La$_2$W$_{1.7}$Mo$_{0.3}$O$_9$ is similar to that of β-La$_2$Mo$_2$O$_9$. Even the occupancies of O2 and O3 are quite similar although the errors are high due to the dominant scattering power of the heavy cations. The La–O bond distances range from 2.533(15) to 3.073(12) Å, and
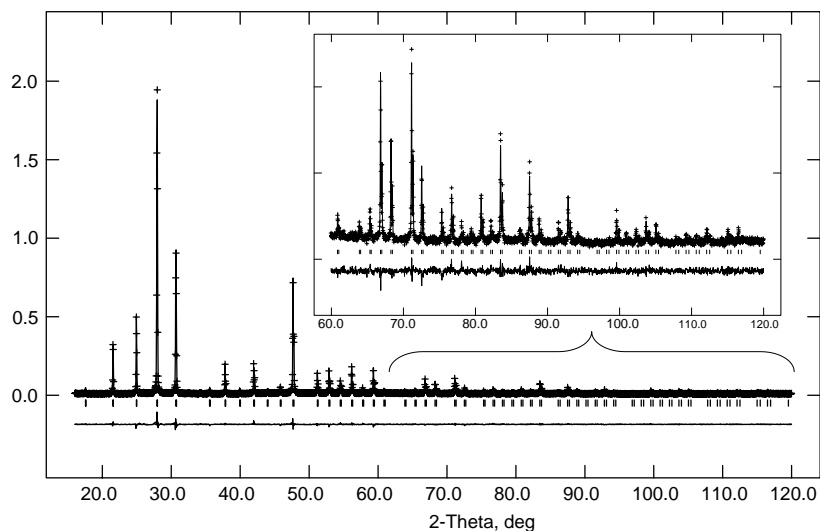

FIG. 4. Laboratory X-ray Rietveld refinement plot for β-La$_2$W$_{1.7}$Mo$_{0.3}$O$_9$ at room temperature.
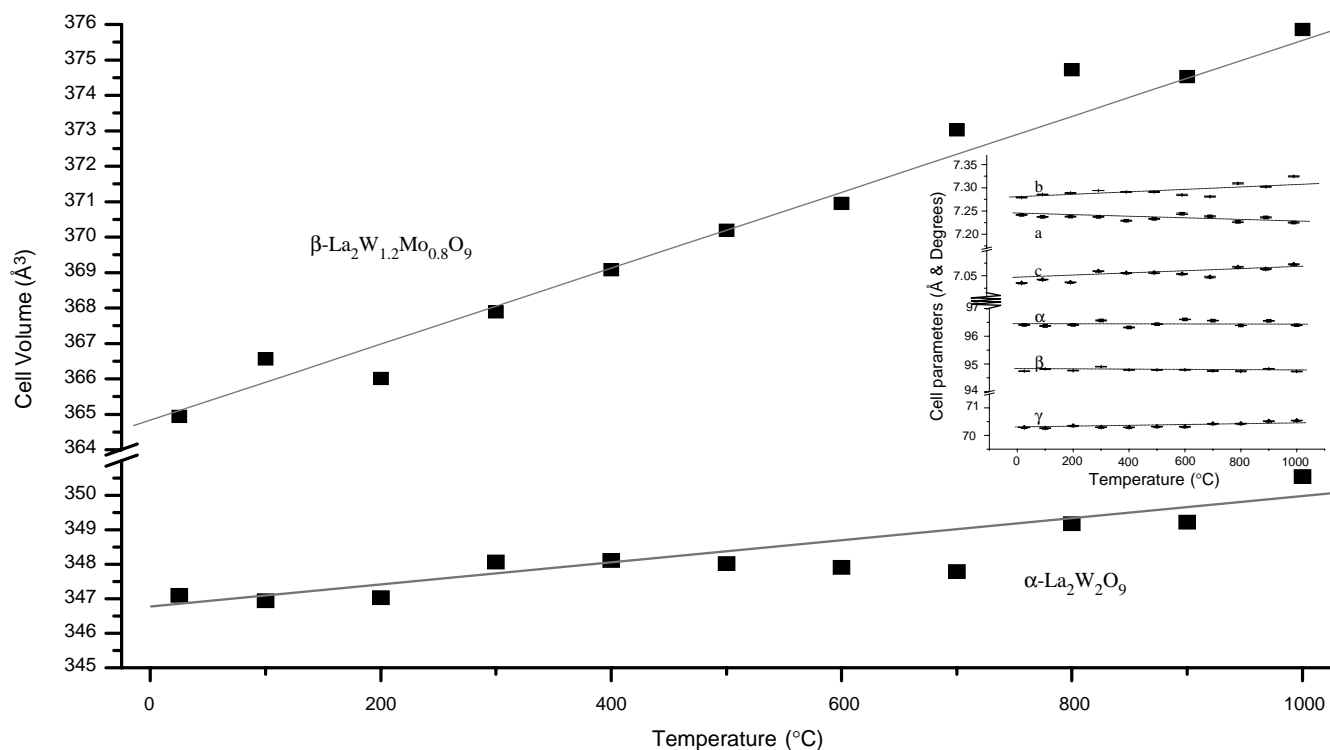
FIG. 5. Thermal expansion curves for β-$La_2W_{1.2}Mo_{0.8}O_9$ (cubic) and α-$La_2W_2O_9$ (triclinic) from LXRP thermodiffractometry. The inset shows the cell parameters evolution for α-$La_2W_2O_9$.

the W/Mo–O bond lengths range between 1.785(9) and 1.841(7) Å.

Thermal Expansion of α and β Forms

We have studied the thermal evolution of some selected stoichiometries, since related compounds display very small (even negative) thermal expansion coefficients. We have recorded the thermodiffractometry of α-$La_2W_2O_9$ as this compound has a very rigid framework (26). The structure is triclinic and we have analyzed the T-variable patterns through the Le Bail's fit to obtain the cell parameters. An approximate linear behavior between RT and 1000°C was obtained. $La_2W_{1.2}Mo_{0.8}O_9$ has also been analyzed as an example of the cubic β structure. This material is single phase and it can be prepared by any type of cooling.

The results of the temperature-dependent studies for both compounds are displayed in Fig. 5, where the unit cell volumes versus temperature are plotted. The inset of that figure shows the triclinic cell parameters evolution. Both cell volumes can be adequately fitted by using the linear expression: $V(T) = n + mT(°C)$. The n and m parameters for triclinic $La_2W_2O_9$ were 346.6(4) and 0.0031(4), respectively. The n and m parameters for cubic $La_2W_{1.2}Mo_{0.8}O_9$ were 364.8(4) and 0.0107(6), respectively. The thermal expansion

coefficients, α_v, defined as $m/3n$, were 2.9×10^{-6} and 9.7×10^{-6}°C^{-1} for α-$La_2W_2O_9$ and β-$La_2W_{1.2}Mo_{0.8}O_9$, respectively. Hence, both compounds show positive thermal expansion although the value for α-$La_2W_2O_9$ is quite small and it can be classified as a low positive thermal expansion material.

REFERENCES

1. Ph. Lacorre, *Solid State Sci.* **2,** 755 (2000).
2. W. Jeitschko, *Acta Crystallogr. B* **28,** 60 (1972) .
3. J. S. O. Evans, T. A. Mary, and A. W. Sleight, *J. Solid State Chem.* **133,** 580 (1997) .
4. A. Moini, M. A. Subramanian, A. Clearfield, F. J. DiSalvo, and W. H. McCaroll, *J. Solid State Chem.* **66,** 136 (1987).
5. T. Mingliang, M. Zhiqiang, and Z. Yuheng, *J. Phys. Condens. Matter* **8,** 3413 (1996).
6. J. E. Greedan, N. P. Raju, A. Wegner, P. Gougeon, and J. Padiou, *J. Solid State Chem.* **129,** 320 (1997).
7. H. Kerner-Czeskleba and G. Tourné, *Mater. Res. Bull.* **13,** 271 (1978).

8. J. Gopalakrishnan and A. Manthiram, *J. Chem. Soc. Dalton Trans.* 668 (1981).

9. M. Ledesert, Ph. Labbé, W. H. McCaroll, H. Leligny, and B. Raveau, *J. Solid State Chem.* **105,** 143 (1993).

10. Ph. Lacorre, F. Goutenoire, O. Bohnke, R. Retoux, and Y. Laligant, *Nature* **404,** 856 (2000).

11. F. Goutenoire, O. Isnard, E. Suard, O. Bohnke, Y. Laligant, R. Retoux, and Ph. Lacorre, *J. Mater. Chem.* **11,** 119 (2001).

12. F. Goutenoire, O. Isnard, R. Retoux, and Ph. Lacorre, *Chem. Mater*. **12,** 2575 (2000).

13. K. R. Kendall, C. Navas, J. K. Thomas, and H.-C. zur Loye, *Solid State Ionics* **82,** 215 (1995).

14. T. Ishihara, H. Matsuda, and Y. Takita, *J. Am. Chem. Soc.* **116,** 3801 (1994).

15. M. Feng and J. B. Goodenough, *Eur. J. Solid State Inorg. Chem.* **31,** 663 (1994).

16. E. C. Subbarao, A. H. Heuer, and L. W. Hobbs, Eds., "Science and Technology of Zirconia I," Vol. 3. American Ceramic Society, Columbus, OH, pp. 1–24, 1981.

17. H. L. Tuller, *Solid State Ionics* **94,** 63 (1997).

18. S. A. Kramer and H. L. Tuller, *Solid State Ionics* **82,** 15 (1995).

19. F. Abraham, M. F. Debreuille-Gresse, G. Mairesse, and G. Nowogrocki, *Solid State Ionics* **28–30,** 529 (1988).

20. F. Abraham, J. C. Boivin, G. Mairesse, and G. Nowogrocki, *Solid State Ionics* **40–41,** 934 (1990).

21. G. I. Tyudhevskaya, N. S. Afonskii, and V. I. Spityn, *Dokl. Akad Nauk SSSR* **170,** 859 (1966).

22. E. Yarode and V. N. Karpov, *Neorg. Mater*. **2,** 583 (1966).

23. M. M. Ivanova, G. M. Balagina, and E. Yarode, *Neorg. Mater* **6,** 914 (1966).

24. A. V. Kovalesky, V. V. Kharton, and E. N. Naumovich, *Mater. Lett.* **38,** 300 (1999).

25. M. Yoshimura and A. Rouanet, *Mater. Res. Bull.* **11,** 151–158 (1976).

26. Y. Laliglant, A. Le Bail, and F. Goutenoire, *J. Solid State Chem.* **159,** 223 (2001).

27. J. S. O. Evans, T. A. Mary, T. Vogt, M. A. Subramanian, and A. W. Sleight, *Chem. Mater*. **8,** 2811 (1996).

28. C. Lind, A. P. Wilkinson, Z. B. Hu, S. Short, and J. D. Jorgensen, *Chem. Mater*. **10,** 2335 (1998).

29. C. Lind, D. G. Vanderveer, A. P. Wilkinson, J. H. Chen, M. T. Vaughan, and D. J. Weidner, *Chem. Mater*. **13,** 487–490 (2001).

30. C. Closmann, J. Haygarth, and A. W. Sleight, *J. Solid State Chem.* **139,** 424 (1998).

31. J. S. O. Evans, T. A. Mary, and A. W. Sleight, *J. Solid State Chem.* **133,** 580 (1997).

32. K. J. Rao, B.Vidhyanathan, M. Ganguli, and P. A. Ramakrishnan, *Chem. Mater*. **11,** 882 (1999).

33. K. J. Rao and P. D. Ramesh, *Bull. Mater. Sci*. **18,** 447 (1995).

34. D. M. P. Mingos and D. R. Baghurst, *Chem. Soc. Rev*. **20,** 1 (1991).

35. D. E. Clark and W. H. Suttom, *Annu. Rev. Mater. Sci*. **26,** 299 (1996).

36. M. P. Selvam and K. J. Rao, *Adv. Mater*. **12,** 1621 (2000).

37. R. A. Young, The Rietveld Method, Oxford University Press, Oxford, 1993.

38. T. I. Bylichkina, L. I. Soleva, E. A. Pobedimskaya, M. A. Porai-Koshits, and N. V. Belov, *Kristallografiya* **15,** 165–167 (1970).